Journal of Multidisciplinary Engineering Science and Technology (JMEST)
ISSN: 2458-9403
Vol. 13 Issue 7, July - 2026

Personalized 3D-Printed Atenolol For Infantile Hemangioma

Francisco José Raposo
Nupics, Federal University of Juiz de Fora
Juiz de Fora, Brazi

Débora Brandão Barbosa
Nupics, Federal University of Juiz de Fora
Juiz de Fora, Brazil

Marcos dos Reis Casarim
Nupics, Federal University of Juiz de Fora
Juiz de Fora, Brazil

Nádia Rezende Barbosa Raposo
Nupics, Faculty of Pharmacy, Federal University of Juiz de Fora
Juiz de Fora, Brazi

Marcos Antônio Fernandes Brandão
Nupics, Faculty of Pharmacy, Federal University of Juiz de Fora
Juiz de Fora, Brazi

Abstract— This study developed and characterised a three-dimensional (3D) printing platform to produce personalised oral atenolol dosage forms intended for paediatric patients with infantile haemangioma. Pharmaceutical scaffolds were designed by computer-aided design (CAD) and manufactured by fused deposition modelling (FDM) using poly(lactic acid) (PLA), polyvinyl alcohol (PVA), and thermoplastic polyurethane (TPU). The scaffold geometry was parametrically adjusted to enable personalised drug loading through an automated semi-solid dispensing system controlled by proprietary G-code. Printing performance, dimensional accuracy, mass uniformity, drug-loading efficiency, and atenolol content were evaluated. Among the tested polymers, PLA exhibited the highest dimensional fidelity and reproducibility, with the lowest variability for internal diameter (CV = 0.35%), depth (CV = 0.31%), wall thickness (CV = 0.95%), and scaffold mass (147.35 ± 1.66 mg; CV = 1.13%), justifying its selection for subsequent experiments. PLA also provided the shortest printing time (21 min 39 s), while material consumption remained constant (0.20 g per scaffold) across all polymers. Automated drug loading achieved a mean mass gain of 99.70 ± 5.03%, corresponding to a loading efficiency of 92.66 ± 4.67%, demonstrating effective drug incorporation into the printed scaffolds. Atenolol quantification by UV–Vis spectrophotometry showed a mean drug content of 92.26 ± 3.81% (CV = 4.13%), confirming satisfactory dose uniformity and manufacturing reproducibility. Overall, the proposed platform integrates digital design, FDM printing, and automated semi-solid dispensing into a reproducible workflow capable of producing personalised oral dosage forms. These findings indicate the technical feasibility of the proposed platform and suggest that additive manufacturing may offer a promising approach for producing personalised paediatric medicines requiring individualised dose adjustment.

Keywords*— 3D *printing; atenolol; infantile hemangioma; automation; personalized treatment.

I. INTRODUCTION

Precision medicine has challenged the traditional “one-size-fits-all” approach by recognizing that patient-specific factors, including age, body weight, genetic background, metabolic status, disease characteristics, and drug response, critically influence therapeutic efficacy and safety [1]. Advances in pharmacogenomics and translational medicine have driven the development of individualized treatment strategies designed to optimize therapeutic outcomes according to each patient’s clinical profile [2].

Within this context, three-dimensional (3D) printing has emerged as a transformative technology for personalized pharmacotherapy, enabling the on-demand fabrication of patient-specific dosage forms from computer-aided design (CAD) models. This approach allows precise control overdose, geometry, formulation composition, and drug-release profiles, supporting flexible and decentralized pharmaceutical manufacturing [3-4]. Among additive manufacturing platforms, fused deposition modeling (FDM) and material extrusion technologies have gained prominence due to their accessibility, cost-effectiveness, and compatibility with diverse pharmaceutical polymers and drug-loaded systems [5-6]. Recent advances have demonstrated the ability of extrusion-based printing to produce complex dosage forms with programmable release characteristics, including pediatric formulations through hot-melt extrusion integration and personalized drug-delivery [7-9]. These innovations reinforce the translational potential of additive manufacturing for patient-centered therapies, particularly for populations requiring individualized dosing strategies [10-11]. The clinical relevance of this approach becomes evident in pediatric diseases, where limited availability of age-appropriate formulations frequently requires manipulation of adult

dosage forms, compromising dose accuracy and treatment precision.

Infantile hemangioma, the most common benign vascular tumor of infancy, highlights the need for individualized pharmacotherapy. Atenolol has emerged as an effective alternative to propranolol because of its β1-selectivity, comparable efficacy, and favorable safety profile, with clinical studies—including a 46-infant case series and recent Brazilian experience—reporting successful treatment and good tolerability [12-14]. However, the lack of age-appropriate formulations necessitates tablet manipulation, a practice associated with inaccurate pediatric dosing and substantial variability in atenolol content after tablet splitting [15-16].

Accordingly, this study aimed to develop and characterize an FDM-based pharmaceutical platform for manufacturing personalized oral dosage forms containing atenolol to support individualized treatment of pediatric patients with infantile hemangioma.

II. Material and Method

A. Three-dimensional scaffold design

Pharmaceutical scaffolds were designed using a computer-aided design (CAD) environment through parametric modelling to enable precise control of scaffold geometry and internal architecture. The design incorporated adjustable geometric parameters, including length, width, height, wall thickness, internal cavity dimensions, and internal volume, allowing modulation of the available loading space according to the intended atenolol dose for paediatric patients with infantile haemangioma. The validated digital models were exported as Standard Tessellation Language (STL) files to preserve geometric fidelity and ensure compatibility with the additive manufacturing workflow. The STL files were subsequently imported into Bambu Studio v2.6.0.51 (Bambu Lab) for definition of the printing configuration and generation of the fabrication toolpaths.

B. Scaffold fabrication by FDM

Pharmaceutical scaffolds were fabricated by FDM using a desktop 3D printer (Bambu Lab A1). Fabrication was performed through layer-by-layer deposition of thermoplastic filaments according to the predefined CAD models and printing parameters generated by the slicing software. Poly(lactic acid) (PLA), poly(vinyl alcohol) (PVA), and thermoplastic polyurethane (TPU) filaments (1.75 mm diameter) were evaluated as printing materials. Before printing, filaments were dried to minimise moisture-related variations during extrusion. Drying conditions were selected according to the hygroscopic characteristics of each polymer: PLA was dried at 45 °C for 6 h, PVA at 55 °C for 12 h, and TPU at 55 °C for 8 h. Printing parameters, including layer height, line width, printing speed, nozzle temperature, build-plate temperature, infill pattern, infill density, number of perimeters, and support generation, were adjusted according to the characteristics of each polymer. Fabricated scaffolds were subsequently evaluated regarding dimensional accuracy, structural fidelity, mass uniformity, printing time, and material consumption.

The printing parameters were optimised for each thermoplastic filament evaluated. All scaffolds were fabricated using a layer height of 0.20 mm. The line width parameters were defined as follows: initial layer width of 0.50 mm, external wall width of 0.42 mm, internal wall width of 0.45 mm, top surface width of 0.42 mm, and internal solid infill width of 0.42 mm for PLA and 0.45 mm for both PVA and TPU. Regarding precision parameters, the slicing configuration used a gap-closing radius of 0.049 mm and a resolution of 0.012 mm for all evaluated filaments. Structural parameters were standardised across materials, with two wall loops, 15% internal infill density, and a grid infill pattern. Printing speed parameters were maintained constant among the evaluated polymers, with an initial layer speed of 50 mm/s, external wall speed of 200 mm/s, and internal wall speed of 300 mm/s. No support structures were generated for any of the evaluated materials. The extrusion temperature was adjusted according to the polymer characteristics, with nozzle temperatures of 190 °C for PLA, 208 °C for PVA, and 210 °C for TPU. The build plate temperature was set at 65 °C for PLA and PVA and 60 °C for TPU. These optimised parameters were used for scaffold fabrication and subsequent evaluation of printability, dimensional accuracy, and structural reproducibility.

C. Development of the automated dispensing platform and customised G-code

Following scaffold fabrication, an automated semi-solid dispensing platform was developed by modifying a BioEnder PRO 3D printer. The conventional extrusion system was replaced with a syringe-based dispensing module to enable controlled deposition of an atenolol-loaded sodium alginate gel into the scaffold cavities. A dedicated positioning device was designed and manufactured to accommodate multiple scaffolds during the dispensing process, ensuring reproducible alignment between the dispensing nozzle and scaffold cavities. A customised computational algorithm was developed to generate specific G-code instructions for the drug-loading stage. The algorithm converted predefined dispensing parameters into automated commands controlling nozzle positioning, dispensing volume, movement speed, and deposition sequence for each scaffold. This approach enabled automated and reproducible incorporation of atenolol into the printed structures according to the predefined loading conditions.

D. Quality assessment of printed scaffolds and pharmaceutical loading

1) Mass characterization and uniformity

Mass uniformity was assessed by individually weighing 20 randomly selected scaffolds using an

analytical balance. Mean mass, standard deviation (SD), coefficient of variation (CV), and relative error (E%) were calculated to evaluate unit-to-unit variability and manufacturing reproducibility. Since specific pharmacopeial requirements for 3D-printed pharmaceutical systems are not yet established, mass variability was interpreted based on general quality principles applied to conventional oral solid dosage forms.

2) Drug loading performance

Drug loading performance was evaluated by determining scaffold mass variation after atenolol incorporation. Each unit (n = 20) was weighed before and after drug loading, and the incorporated mass was calculated from the difference between loaded and unloaded scaffolds. Loading efficiency was calculated as the percentage ratio between the experimentally incorporated amount of atenolol and the theoretical drug amount defined by the digital design.

3) Atenolol content analysis

Atenolol content was determined by UV–Vis spectrophotometry using a previously established calibration curve. The analytical method was evaluated based on linearity, and the drug content was expressed as mean percentage of the labelled amount.

III. RESULTS AND DISCUSSION

The pharmaceutical scaffold was successfully designed using a parametric CAD-based workflow, with the technical drawing defining the geometric configuration and structural features of the proposed system (Figure I).

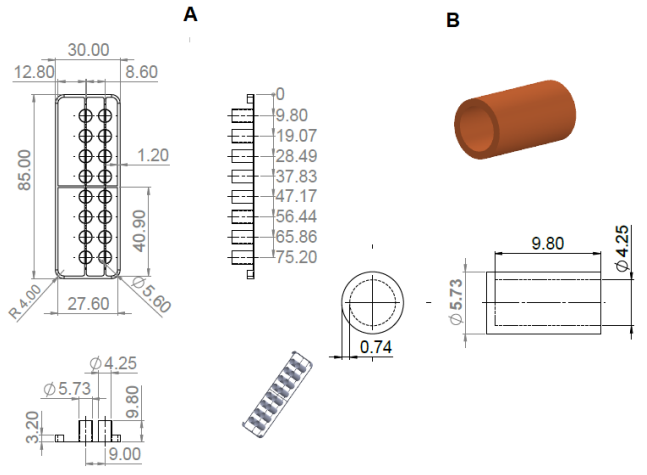

FIG I. DIGITAL DESIGN OF THE SCAFFOLD FOR ORAL DOSAGE FORM FABRICATION (A – 16-UNIT ARRAY AND B – INDIVIDUAL SCAFFOLD) USING FUSED DEPOSITION MODELLING-BASED 3D PRINTING.

The digital model allowed adjustment of key geometric parameters, including external dimensions, wall thickness, cavity geometry, and internal volume, providing flexibility for modulation of scaffold loading capacity according to formulation requirements. The scaffold architecture was designed to support FDM fabrication and subsequent semi-solid loading of atenolol, with adjustable internal volume to accommodate different drug-loading requirements. This design strategy was developed to address the need for individualised dosing approaches in paediatric patients with infantile haemangioma, where atenolol therapy may require dose adjustment based on patient-specific factors, including body weight.

PLA, PVA, and TPU were evaluated as candidate polymers for scaffold fabrication. Dimensional characteristics and mass uniformity were assessed using 20 scaffolds produced from each material. PLA exhibited the highest dimensional reproducibility, with the lowest variability in internal diameter (4.10 ± 0.01 mm; CV = 0.35%), depth (9.69 ± 0.03 mm; CV = 0.31%), and wall thickness (0.75 ± 0.01 mm; CV = 0.95%). In comparison, PVA showed greater dimensional variability, particularly in wall thickness (0.88 ± 0.04 mm; CV = 4.03%), whereas TPU exhibited the highest variation (0.61 ± 0.05 mm; CV = 8.10%).

Mass analysis confirmed the superior reproducibility of PLA scaffolds, which presented a mean mass of 147.35 ± 1.66 mg (CV = 1.13%; relative error = 1.60%), compared with PVA (143.70 ± 7.78 mg; CV = 5.41%; relative error = 3.19%) and TPU (146.70 ± 5.91 mg; CV = 4.03%; relative error = 4.28%).

The higher reproducibility observed for PLA was consistent with its greater geometric fidelity to the CAD model, whereas PVA and TPU exhibited higher structural variability. These findings are consistent with the physicochemical characteristics of these polymers, as PLA generally provides greater rigidity and dimensional stability during FDM processing, while TPU flexibility and PVA hygroscopicity may affect printing precision and structural reproducibility [17–19]. Similar effects of polymer properties on FDM printability and pharmaceutical product quality have been previously reported [20–22]. Based on dimensional accuracy and mass reproducibility, PLA was selected for subsequent atenolol loading experiments.

Printing time and material consumption were evaluated under the optimized printing conditions for each polymer. PLA showed the shortest fabrication time (21 min 39 s), followed by PVA (24 min 19 s) and TPU (27 min 33 s). Material consumption was identical for all polymers, averaging 0.20 g per scaffold. These findings highlight the relevance of process efficiency parameters in the optimization of additive manufacturing workflows, particularly when considering scalability and implementation in decentralized pharmaceutical production. Reduced printing time and consistent material consumption contribute to the optimisation of additive manufacturing workflows by improving process efficiency and resource utilisation. These characteristics are aligned with sustainable manufacturing principles and the objectives of the United Nations Sustainable Development Goal 12 (Responsible Consumption and Production), which promotes more efficient production systems and reduced resource waste [23,24].

Furthermore, the digital and layer-by-layer manufacturing approach adopted in this study is consistent with the ISO/ASTM 52900:2021 framework, which defines additive manufacturing processes and supports the classification of extrusion-based fabrication technologies used to produce three-dimensional objects from digital models [25].

A customised G-code enabled the automated deposition of atenolol-loaded sodium alginate gel into 16-well PLA pharmaceutical scaffolds, providing control over dispensing parameters and improving loading process reproducibility. The printed scaffolds exhibited high mass uniformity (CV and relative error <2%), indicating consistency of the fabrication process. Following automated drug incorporation, the PLA scaffolds exhibited a mean mass gain of 99.70 ± 5.03% (CV = 5.04%; relative error = 7.34%) and a loading efficiency of 92.66 ± 4.67% (CV = 5.04%). These results indicate effective incorporation of atenolol into the scaffold cavities and satisfactory reproducibility of the loading process under the evaluated experimental conditions. The observed performance is consistent with previous reports describing post-print drug-loading strategies in 3D-printed pharmaceutical systems [26–29]. Overall, the developed automated semi-solid dispensing approach enabled reproducible atenolol incorporation into FDM-printed scaffolds, providing a technological basis for further investigation of personalised oral dosage forms requiring dose adjustment.

The atenolol content in the printed scaffolds was determined by UV–Vis spectrophotometry using an analytical calibration curve ($y = 0.0194x + 0.0499$). The method showed linearity up to 50 µg/mL, with a coefficient of determination (R^2) of 0.995. The mean atenolol content was 92.26 ± 3.81%, with a CV of 4.13% (Table I), indicating adequate homogeneity among the printed units and low variability in the drug incorporation process. Although specific acceptance criteria for 3D-printed dosage forms have not yet been established, the obtained drug content values fall within the range commonly accepted for conventional atenolol solid dosage forms (approximately 90–110% of labelled content) according to the Brazilian Pharmacopoeia [30]. Therefore, the observed variability supports the reproducibility of the developed prototype under the evaluated conditions.

TABLE I. ATENOLOL CONTENT DETERMINATION IN 3D-PRINTED SCAFFOLDS BY UV–VIS SPECTROPHOTOMETRY.

Samples (printed capsules)	Atenolol content (%)
1	89.5
2	92.1
3	93.6
4	96.2
5	92.1
6	85.2
7	94.2
8	91.1
9	98.9
10	89.7
Mean	**92.26**
Standard deviation (SD)	**3.81**
Coefficient of variation (CV, %)	**4.13**

IV. CONCLUSION

This study demonstrated the technical feasibility of a 3D printing platform for the development of personalised oral atenolol dosage forms intended for paediatric applications in infantile haemangioma. Parametric PLA scaffolds enabled control of internal geometry and loading capacity, while the automated semi-solid dispensing system allowed reproducible incorporation of atenolol into the printed structures.

The fabricated dosage forms exhibited satisfactory quality attributes, including dimensional reproducibility, mass uniformity, loading efficiency, and atenolol content consistency. These findings indicate that the combination of FDM-based scaffold fabrication and automated drug dispensing represents a promising approach for the development of personalised pharmaceutical systems requiring dose adjustment.

Further studies involving different dose levels, formulation optimisation, stability assessment, and *in vitro* or clinical performance evaluation are required to advance the application of this technology in personalised paediatric medicine.

ACKNOWLEDGMENT

D.B.R. and M.R.C. gratefully acknowledge the financial support provided through master's scholarships from CAPES. The authors also thank the Graduate Program in Health at the Federal University of Juiz de Fora, Brazil, for its institutional support.

REFERENCES

[1] Iriart JAB. Precision medicine/personalized medicine: a critical analysis of movements in the transformation of biomedicine in the early 21st century. *Cadernos de Saúde Pública*. 2019;35(3):e00153118. doi:10.1590/0102-311X00153118.

[2] Marques-Garcia F, Martinez-Bravo C. A review of pharmacogenomics in the individualization of pharmacological treatment: present and future. *Journal of Laboratory and Precision Medicine*. 2026;11:6. doi:10.21037/jlpm-25-9.

[3] Trenfield SJ, Awad A, Goyanes A, Gaisford S, Basit AW. 3D printing pharmaceuticals: Drug development to frontline care. *Trends in Pharmacological Sciences.* 2018;39(5):440-451. doi:10.1016/j.tips.2018.02.006.

[4] Seoane-Viaño I, Januskaite P, Catani M, Trenfield SJ, Goyanes A, Basit AW. Semi-solid extrusion 3D printing in drug delivery and personalized medicine. *Advanced Drug Delivery Reviews*. 2021;174:659-675. doi:10.1016/j.addr.2021.04.013.

[5] Goyanes A, Kobayashi M, Martínez-Pacheco R, Gaisford S, Basit AW. Fused-filament 3D printing of drug products: microstructure analysis and drug release characteristics of PVA-based caplets. *International Journal of Pharmaceutics*.

2016;514(1):290-5. doi:10.1016/j.ijpharm.2016.06.021.
[6] Auriemma G, Tommasino C, Falcone G, Esposito T, Sardo C, Aquino RP. Additive manufacturing strategies for personalized drug delivery systems and medical devices: fused filament fabrication and semi-solid extrusion. *Molecules*. 2022;27(9):2784. doi:10.3390/molecules27092784.
[7] Paccione N, Guarnizo-Herrero V, Ramalingam M, Larrarte E, Pedraz JL. Application of 3D printing on the design and development of pharmaceutical oral dosage forms. *Journal of Controlled Release*. 2024;373:463-480. doi:10.1016/j.jconrel.2024.07.035.
[8] Kolipaka SS, Junqueira LA, Garg V, Trivedi V, Douroumis D. Continuous manufacturing of 3D-printed chewable pediatric gummies by coupling hot melt extrusion with direct extrusion additive manufacturing. *Expert Opinion on Drug Delivery*. 2026. doi:10.1080/17425247.2026.2636173.
[9] Junqueira LA, Ghanizadeh Tabriz A, Koltsakidis S, Tzetzis D, Raposo FJ, Douroumis D, Brandão MAF, Raposo NRB. 3D polyurethane vaginal rings for the delivery of steroid hormones using material extrusion additive manufacturing. *International Journal of Pharmaceutics*. 2026; 699:127004. doi:10.1016/j.ijpharm.2026.127004.
[10] Goyanes A, Madla CM, Umerji A, Duran Piñeiro G, Giraldez Montero JM, Lamas Diaz MJ, et al. Automated therapy preparation of isoleucine formulations using 3D printing for the treatment of maple syrup urine disease. *International Journal of Pharmaceutics*. 2019; 567:118497. doi:10.1016/j.ijpharm.2019.118497.
[11] Casarim MDR, Raposo NRB, Raposo FJ, Vaz UP, Brandão MAF. 3D printing of scaffolds with fluoxetine hydrochloride for personalized depression therapy. *Journal of Multidisciplinary Engineering Science and Technology (JMEST).* 2026;13(2). ISSN 2458-9403.
[12] Chen T, Gudipudi R, Nguyen SA, Carroll W, Clemmens C. Should Propranolol Remain the Gold Standard for Treatment of Infantile Hemangioma? A Systematic Review and Meta-Analysis of Propranolol Versus Atenolol. *Otolaryngology–Head and Neck Surgery*. 2023;168(3). doi:10.1177/00034894221089758.
[13] Calderón-Castrat X, Velásquez F, Castro R, Ballona R. Oral atenolol for infantile hemangioma: case series of 46 infants. *Actas Dermo-Sifiliográficas (English Edition).* 2020;111(1):59-62. doi:10.1016/j.adengl.2019.11.004.
[14] Rocha TOC, Berenguer NDB, Martins CBV, Bessa VR, Samorano LP, Rivitti-Machado MC, Oliveira ZNP. Brazilian experience with oral atenolol in the treatment of infantile hemangiomas. *Anais Brasileiros de Dermatologia.* 2025;100(1):141-145. doi:10.1016/j.abd.2024.03.013.
[15] Auricchio MT, Yano HM, Santos AP, Bugno A. Avaliação do teor de Atenolol em comprimidos divididos com faca caseira e aparelho cortador. *Acta Paulista de Enfermagem*. 2011;24(1):74-79. doi:10.1590/S0103-21002011000100011.
[16] Nguyen D, Secretan PH, Auvity S, Vidal F. Assessment of practices for suspended oral drugs by tablet crushing in pediatric units. *European Journal of Pharmaceutics and Biopharmaceutics*. 2020;157:175-182. doi:10.1016/j.ejpb.2020.10.013.
[17] Farah S, Anderson DG, Langer R. Physical and mechanical properties of PLA, and their functions in widespread applications — A comprehensive review. *Adv Drug Deliv Rev*. 2016;107:367-392. doi:10.1016/j.addr.2016.06.012.
[18] Ngo TD, Kashani A, Imbalzano G, Nguyen KTQ, Hui D. Additive manufacturing (3D printing): A review of materials, methods, applications and challenges. *Compososites* Part B Eng. 2018;143:172-196. doi:10.1016/j.compositesb.2018.02.012.
[19] Dizon JRC, Espera AH Jr, Chen Q, Advincula RC. Mechanical characterization of 3D-printed polymers. *Additive Manufacturing*. 2018;20:44-67. doi:10.1016/j.addma.2017.12.002.
[20] Goyanes A, Buanz ABM, Hatton GB, Gaisford S, Basit AW. 3D printing of modified-release aminosalicylate (4-ASA and 5-ASA) tablets. *European Journal of Pharmaceutics and Biopharmaceutics*. 2015;89:157-162. doi:10.1016/j.ejpb.2014.12.003.
[21] Tagami T, Fukushige K, Ogawa E, Hayashi N, Ozeki T. 3D printing factors important for the fabrication of polyvinyl alcohol filament-based tablets. Biol Pharm Bull. 2017;40:357-64. doi: 10.1248/bpb.b16-00878.
[22] Jamróz W, Szafraniec J, Kurek M, Jachowicz R. 3D printing in pharmaceutical and medical applications: recent achievements and challenges. *Pharmaceutical Research*. 2018;35(9):176. doi:10.1007/s11095-018-2454-x).
[23] Gebler M, Uiterkamp AJMS, Visser C. A global sustainability perspective on 3D printing technologies. *Energy Policy.* 2014;74:158-167. doi:10.1016/j.enpol.2014.08.033.
[24] United Nations. *Transforming our world: the 2030 Agenda for Sustainable Development.* New York: United Nations; 2015.
[25] International Organization for Standardization; ASTM International. *ISO/ASTM 52900:2021: Additive manufacturing — General principles — Fundamentals and vocabulary.* Geneva: International Organization for Standardization; 2021.
[26] ICH Q8 (R2) – Quality by Design International Council for Harmonisation of Technical Requirements for Pharmaceuticals for Human Use (ICH). Pharmaceutical development Q8(R2). Geneva: ICH; 2009. Available from: https://www.ich.org/page/quality-guidelines.
[27] Thanawuth K, Sutthapitaksakul L, Konthong S, Suttiruengwong S, Huanbutta K, Dass CR, Sriamornsak P. Impact of drug loading method on drug release from 3D-printed tablets made from filaments fabricated by hot-melt extrusion and impregnation processes. *Pharmaceutics*. 2021;13(10):1607. doi:10.3390/pharmaceutics13101607.

[28] Saviano M, Bowles BJ, Penny MR, Ishaq A, Muwaffak Z, Falcone G, Russo P, Hilton ST. Development and analysis of a novel loading technique for FDM 3D printed systems: microwave-assisted impregnation of gastro-retentive PVA capsular devices. International Journal of Pharmaceutics. 2022;613:121386. doi:10.1016/j.ijpharm.2021.121386.

[29] Ahmed Y, Mahmoud AAK, Ludasi K, Sovány T. Advances in loading techniques and quality by design for fused deposition modeling in pharmaceutical production: a systematic review. *Pharmaceuticals* (Basel). 2024;17(11):1496. doi:10.3390/ph17111496.

[30] Brazilian Health Regulatory Agency (ANVISA). *Brazilian Pharmacopoeia.* 6th ed. Brasília: Brazilian Health Regulatory Agency; 2019. 2 vol.